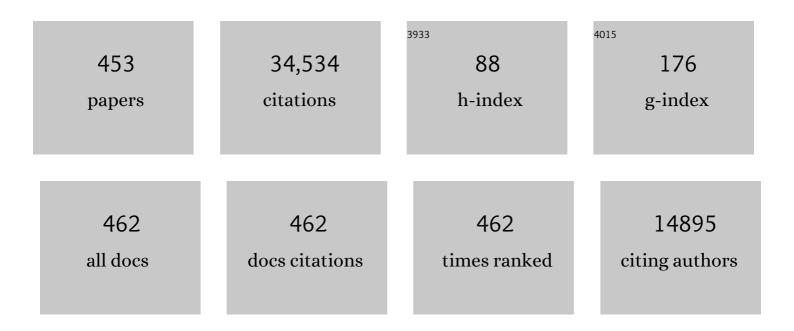
List of Publications by Year in descending order

Source: https://exaly.com/author-pdf/7478606/publications.pdf Version: 2024-02-01



#	Article	IF	CITATIONS
1	Automatic Landslide Inventory Mapping Approach Based on Change Detection Technique With Very-High-Resolution Images. IEEE Geoscience and Remote Sensing Letters, 2022, 19, 1-5.	3.1	7
2	BS-McL: Bilevel Segmentation Framework With Metacognitive Learning for Detection of the Power Lines in UAV Imagery. IEEE Transactions on Geoscience and Remote Sensing, 2022, 60, 1-12.	6.3	8
3	Training Samples Enriching Approach for Classification Improvement of VHR Remote Sensing Image. IEEE Geoscience and Remote Sensing Letters, 2022, 19, 1-5.	3.1	3
4	Land Cover Change Detection Techniques: Very-high-resolution optical images: A review. IEEE Geoscience and Remote Sensing Magazine, 2022, 10, 44-63.	9.6	101
5	Novel Automatic Approach for Land Cover Change Detection by Using VHR Remote Sensing Images. IEEE Geoscience and Remote Sensing Letters, 2022, 19, 1-5.	3.1	5
6	Asymmetric Hash Code Learning for Remote Sensing Image Retrieval. IEEE Transactions on Geoscience and Remote Sensing, 2022, 60, 1-14.	6.3	22
7	Object-Based Sorted-Histogram Similarity Measurement for Detecting Land Cover Change With VHR Remote Sensing Images. IEEE Geoscience and Remote Sensing Letters, 2022, 19, 1-5.	3.1	9
8	Simple Multiscale UNet for Change Detection With Heterogeneous Remote Sensing Images. IEEE Geoscience and Remote Sensing Letters, 2022, 19, 1-5.	3.1	38
9	Predicting Classification Performance for Benchmark Hyperspectral Datasets. IEEE Journal of Selected Topics in Applied Earth Observations and Remote Sensing, 2022, 15, 4180-4193.	4.9	1
10	A General Spline-Based Method for Centerline Extraction from Different Segmented Road Maps in Remote Sensing Imagery. Remote Sensing, 2022, 14, 2074.	4.0	1
11	A Pan-Sharpening Method with Beta-Divergence Non-Negative Matrix Factorization in Non-Subsampled Shear Transform Domain. Remote Sensing, 2022, 14, 2921.	4.0	6
12	Scheduling-Guided Automatic Processing of Massive Hyperspectral Image Classification on Cloud Computing Architectures. IEEE Transactions on Cybernetics, 2021, 51, 3588-3601.	9.5	54
13	Iterative Training Sample Expansion to Increase and Balance the Accuracy of Land Classification From VHR Imagery. IEEE Transactions on Geoscience and Remote Sensing, 2021, 59, 139-150.	6.3	57
14	Local Histogram-Based Analysis for Detecting Land Cover Change Using VHR Remote Sensing Images. IEEE Geoscience and Remote Sensing Letters, 2021, 18, 1284-1287.	3.1	24
15	Change Detection From Very-High-Spatial-Resolution Optical Remote Sensing Images: Methods, applications, and future directions. IEEE Geoscience and Remote Sensing Magazine, 2021, 9, 68-101.	9.6	85
16	Deep Hashing Learning for Visual and Semantic Retrieval of Remote Sensing Images. IEEE Transactions on Geoscience and Remote Sensing, 2021, 59, 9661-9672.	6.3	43
17	Diagnostic Analysis on Change Vector Analysis Methods for LCCD Using Remote Sensing Images. IEEE Journal of Selected Topics in Applied Earth Observations and Remote Sensing, 2021, 14, 10199-10212.	4.9	11
18	Adaptive region-based post-classification framework for land-cover mapping improvement using very high spatial resolution optical imagery. Journal of Applied Remote Sensing, 2021, 15, .	1.3	1

#	Article	IF	CITATIONS
19	A novel optimal multi-pattern matching method with wildcards for DNA sequence. Technology and Health Care, 2021, 29, 115-124.	1.2	2
20	Distributed Computing for Remotely Sensed Data Processing [Scanning the Section]. Proceedings of the IEEE, 2021, 109, 1278-1281.	21.3	1
21	Functional Feature Extraction for Hyperspectral Image Classification With Adaptive Rational Function Approximation. IEEE Transactions on Geoscience and Remote Sensing, 2021, 59, 7680-7694.	6.3	5
22	A Multispectral and Multiangle 3-D Convolutional Neural Network for the Classification of ZY-3 Satellite Images Over Urban Areas. IEEE Transactions on Geoscience and Remote Sensing, 2021, 59, 10266-10285.	6.3	12
23	Practice and Experience in Using Parallel and Scalable Machine Learning in Remote Sensing from HPC Over Cloud to Quantum Computing. , 2021, , .		8
24	Supervised Functional Data Discriminant Analysis for Hyperspectral Image Classification. IEEE Transactions on Geoscience and Remote Sensing, 2020, 58, 841-851.	6.3	11
25	Hyperspectral Mixed Gaussian and Sparse Noise Reduction. IEEE Geoscience and Remote Sensing Letters, 2020, 17, 474-478.	3.1	33
26	Lunar impact crater identification and age estimation with Chang'E data by deep and transfer learning. Nature Communications, 2020, 11, 6358.	12.8	79
27	Object-Oriented Key Point Vector Distance for Binary Land Cover Change Detection Using VHR Remote Sensing Images. IEEE Transactions on Geoscience and Remote Sensing, 2020, 58, 6524-6533.	6.3	38
28	Feature Extraction for Hyperspectral Imagery: The Evolution From Shallow to Deep: Overview and Toolbox. IEEE Geoscience and Remote Sensing Magazine, 2020, 8, 60-88.	9.6	373
29	An Object-Oriented Color Visualization Method with Controllable Separation for Hyperspectral Imagery. Applied Sciences (Switzerland), 2020, 10, 3581.	2.5	3
30	Deep TEC: Deep Transfer Learning with Ensemble Classifier for Road Extraction from UAV Imagery. Remote Sensing, 2020, 12, 245.	4.0	42
31	Spatially Enhanced Spectral Unmixing Through Data Fusion of Spectral and Visible Images from Different Sensors. Remote Sensing, 2020, 12, 1255.	4.0	8
32	Landslide Inventory Mapping With Bitemporal Aerial Remote Sensing Images Based on the Dual-Path Fully Convolutional Network. IEEE Journal of Selected Topics in Applied Earth Observations and Remote Sensing, 2020, 13, 4575-4584.	4.9	27
33	HYPERSPECTRAL AND SPATIALLY ADAPTIVE UNMIXING FOR AN ANALYTICAL RECONSTRUCTION OF FRACTION SURFACES FROM DATA WITH CORRUPTED PIXELS. , 2020, , 209-230.		0
34	Metrological hyperspectral image analysis through spectral differences. , 2020, , 319-340.		0
35	Nomination-favoured opinion pool for optical-SAR-synergistic rice mapping in face of weakened flooding signals. ISPRS Journal of Photogrammetry and Remote Sensing, 2019, 155, 187-205.	11.1	26
36	Novel Adaptive Histogram Trend Similarity Approach for Land Cover Change Detection by Using Bitemporal Very-High-Resolution Remote Sensing Images. IEEE Transactions on Geoscience and Remote Sensing, 2019, 57, 9554-9574.	6.3	63

#	Article	IF	CITATIONS
37	Fusion of Multiple Edge-Preserving Operations for Hyperspectral Image Classification. IEEE Transactions on Geoscience and Remote Sensing, 2019, 57, 10336-10349.	6.3	92
38	Vegetation Cover Estimation Using Convolutional Neural Networks. IEEE Access, 2019, 7, 132563-132576.	4.2	14
39	Novel Land Cover Change Detection Method Based on k-Means Clustering and Adaptive Majority Voting Using Bitemporal Remote Sensing Images. IEEE Access, 2019, 7, 34425-34437.	4.2	79
40	Deep Convolutional Capsule Network for Hyperspectral Image Spectral and Spectral-Spatial Classification. Remote Sensing, 2019, 11, 223.	4.0	77
41	FPA clust: evaluation of the flower pollination algorithm for data clustering. Evolutionary Intelligence, 2019, 14, 1189.	3.6	6
42	Spatial Density Peak Clustering for Hyperspectral Image Classification With Noisy Labels. IEEE Transactions on Geoscience and Remote Sensing, 2019, 57, 5085-5097.	6.3	71
43	Automatic Design of Convolutional Neural Network for Hyperspectral Image Classification. IEEE Transactions on Geoscience and Remote Sensing, 2019, 57, 7048-7066.	6.3	145
44	Deep Learning for Hyperspectral Image Classification: An Overview. IEEE Transactions on Geoscience and Remote Sensing, 2019, 57, 6690-6709.	6.3	977
45	Multisource and Multitemporal Data Fusion in Remote Sensing: A Comprehensive Review of the State of the Art. IEEE Geoscience and Remote Sensing Magazine, 2019, 7, 6-39.	9.6	302
46	A Novel Unsupervised Sample Collection Method for Urban Land-Cover Mapping Using Landsat Imagery. IEEE Transactions on Geoscience and Remote Sensing, 2019, 57, 3933-3951.	6.3	15
47	A Semi-Supervised Approach Towards Land Cover Mapping with Sentinel-2 Desnse Time-Series Imagery. , 2019, , .		0
48	A Class-Oriented Visualization Method for Hyperspectral Imagery. , 2019, , .		0
49	Novel Multi-Scale Filter Profile-Based Framework for VHR Remote Sensing Image Classification. Remote Sensing, 2019, 11, 2153.	4.0	4
50	Remote Sensing Big Data Classification with High Performance Distributed Deep Learning. Remote Sensing, 2019, 11, 3056.	4.0	25
51	Remotely sensed big data: evolution in model development for information extraction [point of view]. Proceedings of the IEEE, 2019, 107, 2294-2301.	21.3	60
52	Hyperspectral Image Classification With Squeeze Multibias Network. IEEE Transactions on Geoscience and Remote Sensing, 2019, 57, 1291-1301.	6.3	79
53	Hierarchical clustering approaches for flood assessment using multi-sensor satellite images. International Journal of Image and Data Fusion, 2019, 10, 28-44.	1.7	6
54	Feature extraction from hyperspectral images using learned edge structures. Remote Sensing Letters, 2019, 10, 244-253.	1.4	9

#	Article	IF	CITATIONS
55	Multisensor Composite Kernels Based on Extreme Learning Machines. IEEE Geoscience and Remote Sensing Letters, 2019, 16, 196-200.	3.1	14
56	Supervised classification methods in hyperspectral imaging—recent advances. Data Handling in Science and Technology, 2019, 32, 247-279.	3.1	5
57	Training sample refining method using an adaptive neighbor to improve the classification performance of very high-spatial resolution remote sensing images. Journal of Applied Remote Sensing, 2019, 13, 1.	1.3	5
58	Landslide Inventory Mapping From Bitemporal High-Resolution Remote Sensing Images Using Change Detection and Multiscale Segmentation. IEEE Journal of Selected Topics in Applied Earth Observations and Remote Sensing, 2018, 11, 1520-1532.	4.9	87
59	Contextual Online Dictionary Learning for Hyperspectral Image Classification. IEEE Transactions on Geoscience and Remote Sensing, 2018, 56, 1336-1347.	6.3	22
60	Extinction Profiles Fusion for Hyperspectral Images Classification. IEEE Transactions on Geoscience and Remote Sensing, 2018, 56, 1803-1815.	6.3	104
61	Hyperspectral Image Denoising With Group Sparse and Low-Rank Tensor Decomposition. IEEE Access, 2018, 6, 1380-1390.	4.2	38
62	Hekla Volcano, Iceland, in the 20th Century: Lava Volumes, Production Rates, and Effusion Rates. Geophysical Research Letters, 2018, 45, 1805-1813.	4.0	19
63	Detection and Correction of Mislabeled Training Samples for Hyperspectral Image Classification. IEEE Transactions on Geoscience and Remote Sensing, 2018, 56, 5673-5686.	6.3	75
64	Generative Adversarial Networks for Hyperspectral Image Classification. IEEE Transactions on Geoscience and Remote Sensing, 2018, 56, 5046-5063.	6.3	497
65	Mapping Urban Areas in China Using Multisource Data With a Novel Ensemble SVM Method. IEEE Transactions on Geoscience and Remote Sensing, 2018, 56, 4258-4273.	6.3	40
66	A modified mean filter for improving the classification performance of very high-resolution remote-sensing imagery. International Journal of Remote Sensing, 2018, 39, 770-785.	2.9	21
67	Joint bilateral filtering and spectral similarity-based sparse representation: A generic framework for effective feature extraction and data classification in hyperspectral imaging. Pattern Recognition, 2018, 77, 316-328.	8.1	59
68	Extended Random Walker for Shadow Detection in Very High Resolution Remote Sensing Images. IEEE Transactions on Geoscience and Remote Sensing, 2018, 56, 867-876.	6.3	55
69	Classification of Multi-Spectral Satellite Image Using Hierarchical Clustering Algorithms. , 2018, , .		0
70	Multi-Scale Object Histogram Distance for LCCD Using Bi-Temporal Very-High-Resolution Remote Sensing Images. Remote Sensing, 2018, 10, 1809.	4.0	16
71	Multi-Scale Structure Extraction for Hyperspectral Image Classification. , 2018, , .		1
72	New Frontiers in Spectral-Spatial Hyperspectral Image Classification: The Latest Advances Based on Mathematical Morphology, Markov Random Fields, Segmentation, Sparse Representation, and Deep Learning. IEEE Geoscience and Remote Sensing Magazine, 2018, 6, 10-43.	9.6	255

#	Article	IF	CITATIONS
73	Of mosses and men: Plant succession, soil development and soil carbon accretion in the sub-Arctic volcanic landscape of Hekla, Iceland. Progress in Physical Geography, 2018, 42, 765-791.	3.2	3
74	Refining Land Cover Classification Maps Based on Dual-Adaptive Majority Voting Strategy for Very High Resolution Remote Sensing Images. Remote Sensing, 2018, 10, 1238.	4.0	21
75	Post-Processing Approach for Refining Raw Land Cover Change Detection of Very High-Resolution Remote Sensing Images. Remote Sensing, 2018, 10, 472.	4.0	46
76	Land Cover Change Detection Based on Adaptive Contextual Information Using Bi-Temporal Remote Sensing Images. Remote Sensing, 2018, 10, 901.	4.0	20
77	Decolorization-Based Hyperspectral Image Visualization. IEEE Transactions on Geoscience and Remote Sensing, 2018, 56, 4346-4360.	6.3	44
78	Sparse Representation-Based Augmented Multinomial Logistic Extreme Learning Machine With Weighted Composite Features for Spectral–Spatial Classification of Hyperspectral Images. IEEE Transactions on Geoscience and Remote Sensing, 2018, 56, 6263-6279.	6.3	32
79	Gaussian Pyramid Based Multiscale Feature Fusion for Hyperspectral Image Classification. IEEE Journal of Selected Topics in Applied Earth Observations and Remote Sensing, 2018, 11, 3312-3324.	4.9	56
80	Simultaneous and Constrained Calibration of Multiple Hyperspectral Images Through a New Generalized Empirical Line Model. IEEE Journal of Selected Topics in Applied Earth Observations and Remote Sensing, 2018, 11, 2047-2058.	4.9	5
81	Interactive multi-image colour visualization for hyperspectral imagery. International Journal of Remote Sensing, 2017, 38, 1062-1082.	2.9	4
82	Oil Spill Detection via Multitemporal Optical Remote Sensing Images: A Change Detection Perspective. IEEE Geoscience and Remote Sensing Letters, 2017, 14, 324-328.	3.1	45
83	Automatic Attribute Profiles. IEEE Transactions on Image Processing, 2017, 26, 1859-1872.	9.8	35
84	From Subpixel to Superpixel: A Novel Fusion Framework for Hyperspectral Image Classification. IEEE Transactions on Geoscience and Remote Sensing, 2017, 55, 4398-4411.	6.3	71
85	A Stepwise Analytical Projected Gradient Descent Search for Hyperspectral Unmixing and Its Code Vectorization. IEEE Transactions on Geoscience and Remote Sensing, 2017, 55, 4925-4943.	6.3	22
86	Developing a general post-classification framework for land-cover mapping improvement using high-spatial-resolution remote sensing imagery. Remote Sensing Letters, 2017, 8, 607-616.	1.4	10
87	Hyperspectral Image Classification via Multiple-Feature-Based Adaptive Sparse Representation. IEEE Transactions on Instrumentation and Measurement, 2017, 66, 1646-1657.	4.7	147
88	Automatic selection of molecular descriptors using random forest: Application to drug discovery. Expert Systems With Applications, 2017, 72, 151-159.	7.6	96
89	PCA-Based Edge-Preserving Features for Hyperspectral Image Classification. IEEE Transactions on Geoscience and Remote Sensing, 2017, 55, 7140-7151.	6.3	273
90	Spatial Technology and Social Media in Remote Sensing: A Survey. Proceedings of the IEEE, 2017, 105, 1855-1864.	21.3	27

JON ATLI BENEDIKTSSON

#	Article	IF	CITATIONS
91	Multiple Kernel Learning for Hyperspectral Image Classification: A Review. IEEE Transactions on Geoscience and Remote Sensing, 2017, 55, 6547-6565.	6.3	194
92	A Novel Methodology to Label Urban Remote Sensing Images Based on Location-Based Social Media Photos. Proceedings of the IEEE, 2017, 105, 1926-1936.	21.3	23
93	Hyperspectral Anomaly Detection With Attribute and Edge-Preserving Filters. IEEE Transactions on Geoscience and Remote Sensing, 2017, 55, 5600-5611.	6.3	291
94	Effective Denoising and Classification of Hyperspectral Images Using Curvelet Transform and Singular Spectrum Analysis. IEEE Transactions on Geoscience and Remote Sensing, 2017, 55, 119-133.	6.3	102
95	Adaptive Spectral–Spatial Compression of Hyperspectral Image With Sparse Representation. IEEE Transactions on Geoscience and Remote Sensing, 2017, 55, 671-682.	6.3	51
96	Hyperspectral Image Classification Using Principal Components-Based Smooth Ordering and Multiple 1-D Interpolation. IEEE Transactions on Geoscience and Remote Sensing, 2017, 55, 1199-1209.	6.3	27
97	Random-Walker-Based Collaborative Learning for Hyperspectral Image Classification. IEEE Transactions on Geoscience and Remote Sensing, 2017, 55, 212-222.	6.3	58
98	Spatial technology and social media in remote sensing: challenges and opportunities [point of view]. Proceedings of the IEEE, 2017, 105, 1583-1585.	21.3	5
99	Tree-based supervised feature extraction method based on self-dual attribute profiles. , 2017, , .		0
100	Spatial Technology and Social Media [Scanning the Issue]. Proceedings of the IEEE, 2017, 105, 1851-1854.	21.3	1
101	Semi-Automatic System for Land Cover Change Detection Using Bi-Temporal Remote Sensing Images. Remote Sensing, 2017, 9, 1112.	4.0	21
102	Iterative clustering based active learning for hyperspectral image classification. , 2017, , .		4
103	Hyperspectral images classification by fusing extinction profiles feature. , 2017, , .		4
104	Simultaneous empirical line calibration of multiple spectral images. , 2017, , .		3
105	Spectral-spatial online dictionary learning for hyperspectral image classification. , 2017, , .		2
106	Multiple composite kernel learning for hyperspectral image classification. , 2017, , .		4
107	Hyperspectral image classification: A benchmark. , 2017, , .		5
108	Automatic Object-Oriented, Spectral-Spatial Feature Extraction Driven by Tobler's First Law of Geography for Very High Resolution Aerial Imagery Classification. Remote Sensing, 2017, 9, 285.	4.0	29

#	Article	IF	CITATIONS
109	Hyperspectral Image Classification With Rotation Random Forest Via KPCA. IEEE Journal of Selected Topics in Applied Earth Observations and Remote Sensing, 2017, 10, 1601-1609.	4.9	93
110	Spectral-Spatial Hyperspectral Image Classification Using Subspace-Based Support Vector Machines and Adaptive Markov Random Fields. Remote Sensing, 2016, 8, 355.	4.0	69
111	A Generalized Image Scene Decomposition-Based System for Supervised Classification of Very High Resolution Remote Sensing Imagery. Remote Sensing, 2016, 8, 814.	4.0	10
112	Novel Object-Based Filter for Improving Land-Cover Classification of Aerial Imagery with Very High Spatial Resolution. Remote Sensing, 2016, 8, 1023.	4.0	15
113	Extinction profiles: A novel approach for the analysis of remote sensing data. , 2016, , .		3
114	Computational Efficiency Active Learning for classification of hyperspectral images. , 2016, , .		1
115	Unsupervised change detection analysis to multi-channel scenario based on morphological contextual analysis. , 2016, , .		7
116	A toolbox for unsupervised change detection analysis. International Journal of Remote Sensing, 2016, 37, 1505-1526.	2.9	20
117	Generalized Differential Morphological Profiles for Remote Sensing Image Classification. IEEE Journal of Selected Topics in Applied Earth Observations and Remote Sensing, 2016, 9, 1736-1751.	4.9	39
118	Hyperspectral Data Classification Using Extended Extinction Profiles. IEEE Geoscience and Remote Sensing Letters, 2016, 13, 1641-1645.	3.1	61
119	Spatial–Spectral Hyperspectral Image Classification Using Random Multiscale Representation. IEEE Journal of Selected Topics in Applied Earth Observations and Remote Sensing, 2016, 9, 4129-4141.	4.9	8
120	Region-based classification of remote sensing images with the morphological tree of shapes. , 2016, , .		3
121	Extinction Profiles for the Classification of Remote Sensing Data. IEEE Transactions on Geoscience and Remote Sensing, 2016, 54, 5631-5645.	6.3	122
122	Probabilistic Fusion of Pixel-Level and Superpixel-Level Hyperspectral Image Classification. IEEE Transactions on Geoscience and Remote Sensing, 2016, 54, 7416-7430.	6.3	71
123	Big Data for Remote Sensing: Challenges and Opportunities. Proceedings of the IEEE, 2016, 104, 2207-2219.	21.3	351
124	Set-to-Set Distance-Based Spectral–Spatial Classification of Hyperspectral Images. IEEE Transactions on Geoscience and Remote Sensing, 2016, 54, 7122-7134.	6.3	52
125	Class-Specific Sparse Multiple Kernel Learning for Spectral–Spatial Hyperspectral Image Classification. IEEE Transactions on Geoscience and Remote Sensing, 2016, 54, 7351-7365.	6.3	60
126	Big Data: Practical Applications [Scanning the Issue]. Proceedings of the IEEE, 2016, 104, 2082-2084.	21.3	2

#	Article	IF	CITATIONS
127	Remote Sensing Image Classification Using Attribute Filters Defined Over the Tree of Shapes. IEEE Transactions on Geoscience and Remote Sensing, 2016, 54, 3899-3911.	6.3	25
128	MTF-Based Deblurring Using a Wiener Filter for CS and MRA Pansharpening Methods. IEEE Journal of Selected Topics in Applied Earth Observations and Remote Sensing, 2016, 9, 2255-2269.	4.9	46
129	ANALYZING REMOTE SENSING IMAGES WITH HIERARCHIAL MORPHOLOGICAL REPRESENTATIONS. , 2016, , 313-330.		0
130	Nonlinear Multiple Kernel Learning With Multiple-Structure-Element Extended Morphological Profiles for Hyperspectral Image Classification. IEEE Transactions on Geoscience and Remote Sensing, 2016, 54, 3235-3247.	6.3	203
131	One-Class Oriented Feature Selection and Classification of Heterogeneous Remote Sensing Images. IEEE Journal of Selected Topics in Applied Earth Observations and Remote Sensing, 2016, 9, 1606-1612.	4.9	36
132	Support Tensor Machines for Classification of Hyperspectral Remote Sensing Imagery. IEEE Transactions on Geoscience and Remote Sensing, 2016, 54, 3248-3264.	6.3	131
133	A novel semi-supervised learning framework for hyperspectral image classification. International Journal of Wavelets, Multiresolution and Information Processing, 2016, 14, 1640005.	1.3	8
134	Class-Separation-Based Rotation Forest for Hyperspectral Image Classification. IEEE Geoscience and Remote Sensing Letters, 2016, 13, 584-588.	3.1	20
135	A Novel Approach for Multispectral Satellite Image Classification Based on the Bat Algorithm. IEEE Geoscience and Remote Sensing Letters, 2016, 13, 599-603.	3.1	88
136	SAR Image Despeckling Via Structural Sparse Representation. Sensing and Imaging, 2016, 17, 1.	1.5	27
137	Spectral–Spatial Adaptive Sparse Representation for Hyperspectral Image Denoising. IEEE Transactions on Geoscience and Remote Sensing, 2016, 54, 373-385.	6.3	119
138	Hyperspectral Image Classification Via Shape-Adaptive Joint Sparse Representation. IEEE Journal of Selected Topics in Applied Earth Observations and Remote Sensing, 2016, 9, 556-567.	4.9	108
139	A Novel Automatic Change Detection Method for Urban High-Resolution Remotely Sensed Imagery Based on Multiindex Scene Representation. IEEE Transactions on Geoscience and Remote Sensing, 2016, 54, 609-625.	6.3	77
140	Quantitative Quality Evaluation of Pansharpened Imagery: Consistency Versus Synthesis. IEEE Transactions on Geoscience and Remote Sensing, 2016, 54, 1247-1259.	6.3	70
141	A novel hierarchical clustering technique based on splitting and merging. International Journal of Image and Data Fusion, 2016, 7, 19-41.	1.7	16
142	An advanced classifier for the joint use of LiDAR and hyperspectral data: Case study in Queensland, Australia. , 2015, , .		0
143	On Scalable Data Mining Techniques for Earth Science. Procedia Computer Science, 2015, 51, 2188-2197.	2.0	6
144	Enabling intelligent copernicus services for carbon and water balance modeling of boreal forest		2

ecosystems & amp; #x2014; North state. , 2015, , .

#	Article	IF	CITATIONS
145	Foreword to the Special Issue on Big Data in Remote Sensing. IEEE Journal of Selected Topics in Applied Earth Observations and Remote Sensing, 2015, 8, 4607-4609.	4.9	2
146	High resolution visible image completion of urban region using corresponding hyperspectral image. , 2015, , .		0
147	An interactive color visualization method with multi-image fusion for hyperspectral imagery. , 2015, , .		4
148	Scalable developments for big data analytics in remote sensing. , 2015, , .		6
149	Automatic morphological attribute profiles. , 2015, , .		1
150	Intrinsic Image Decomposition for Feature Extraction of Hyperspectral Images. IEEE Transactions on Geoscience and Remote Sensing, 2015, 53, 2241-2253.	6.3	148
151	A Novel Feature Selection Approach Based on FODPSO and SVM. IEEE Transactions on Geoscience and Remote Sensing, 2015, 53, 2935-2947.	6.3	98
152	Wavelet-Based Classification of Hyperspectral Images Using Extended Morphological Profiles on Graphics Processing Units. IEEE Journal of Selected Topics in Applied Earth Observations and Remote Sensing, 2015, 8, 2962-2970.	4.9	23
153	Processing high resolution images of urban areas with self-dual attribute filters. , 2015, , .		1
154	Classification of Hyperspectral Images by Exploiting Spectral–Spatial Information of Superpixel via Multiple Kernels. IEEE Transactions on Geoscience and Remote Sensing, 2015, 53, 6663-6674.	6.3	326
155	GPU Implementation of Iterative-Constrained Endmember Extraction from Remotely Sensed Hyperspectral Images. IEEE Journal of Selected Topics in Applied Earth Observations and Remote Sensing, 2015, 8, 2939-2949.	4.9	12
156	A Novel Evolutionary Swarm Fuzzy Clustering Approach for Hyperspectral Imagery. IEEE Journal of Selected Topics in Applied Earth Observations and Remote Sensing, 2015, 8, 2447-2456.	4.9	29
157	Extended Self-Dual Attribute Profiles for the Classification of Hyperspectral Images. IEEE Geoscience and Remote Sensing Letters, 2015, 12, 1690-1694.	3.1	33
158	Spectral–Spatial Classification of Hyperspectral Images With a Superpixel-Based Discriminative Sparse Model. IEEE Transactions on Geoscience and Remote Sensing, 2015, 53, 4186-4201.	6.3	229
159	Challenges and Opportunities of Multimodality and Data Fusion in Remote Sensing. Proceedings of the IEEE, 2015, 103, 1585-1601.	21.3	165
160	Spectral and Spatial Classification of Hyperspectral Images Based on ICA and Reduced Morphological Attribute Profiles. IEEE Transactions on Geoscience and Remote Sensing, 2015, 53, 6223-6240.	6.3	81
161	On Understanding Big Data Impacts in Remotely Sensed Image Classification Using Support Vector Machine Methods. IEEE Journal of Selected Topics in Applied Earth Observations and Remote Sensing, 2015, 8, 4634-4646.	4.9	71
162	A Novel MKL Model of Integrating LiDAR Data and MSI for Urban Area Classification. IEEE Transactions on Geoscience and Remote Sensing, 2015, 53, 5312-5326.	6.3	90

#	Article	IF	CITATIONS
163	Land-cover classification using both hyperspectral and LiDAR data. International Journal of Image and Data Fusion, 2015, 6, 189-215.	1.7	66
164	Model-Based Fusion of Multi- and Hyperspectral Images Using PCA and Wavelets. IEEE Transactions on Geoscience and Remote Sensing, 2015, 53, 2652-2663.	6.3	135
165	A Survey on Spectral–Spatial Classification Techniques Based on Attribute Profiles. IEEE Transactions on Geoscience and Remote Sensing, 2015, 53, 2335-2353.	6.3	312
166	Multiple Feature Learning for Hyperspectral Image Classification. IEEE Transactions on Geoscience and Remote Sensing, 2015, 53, 1592-1606.	6.3	282
167	Feature Selection Based on Hybridization of Genetic Algorithm and Particle Swarm Optimization. IEEE Geoscience and Remote Sensing Letters, 2015, 12, 309-313.	3.1	364
168	Extended Random Walker-Based Classification of Hyperspectral Images. IEEE Transactions on Geoscience and Remote Sensing, 2015, 53, 144-153.	6.3	104
169	Multiple Morphological Profiles From Multicomponent-Base Images for Hyperspectral Image Classification. IEEE Journal of Selected Topics in Applied Earth Observations and Remote Sensing, 2014, 7, 4653-4669.	4.9	53
170	Model based PCA/wavelet fusion of multispectral and hyperspectral images. , 2014, , .		2
171	An ICA based approach to hyperspectral image feature reduction. , 2014, , .		11
172	Morphological Profiles Based on Differently Shaped Structuring Elements for Classification of Images With Very High Spatial Resolution. IEEE Journal of Selected Topics in Applied Earth Observations and Remote Sensing, 2014, 7, 4644-4652.	4.9	45
173	Fusion of hyperspectral and LiDAR data in classification of urban areas. , 2014, , .		10
174	Spectral-spatial hyperspectral classification via shape-adaptive sparse representation. , 2014, , .		0
175	A new framework for hyperspectral image classification using multiple spectral and spatial features. , 2014, , .		7
176	Extended random walkers for hyperspectral image classification. , 2014, , .		2
177	Smart data analytics methods for remote sensing applications. , 2014, , .		8
178	A comparison of self-dual attribute profiles based on different filter rules for classification. , 2014, , .		10
179	Pattern Recognition and Classification. Encyclopedia of Earth Sciences Series, 2014, , 503-509.	0.1	3
180	Spectral–Spatial Hyperspectral Image Classification With Edge-Preserving Filtering. IEEE Transactions on Geoscience and Remote Sensing, 2014, 52, 2666-2677.	6.3	614

#	Article	IF	CITATIONS
181	Spectral–Spatial Classification of Multispectral Images Using Kernel Feature Space Representation. IEEE Geoscience and Remote Sensing Letters, 2014, 11, 288-292.	3.1	65
182	Integration of Segmentation Techniques for Classification of Hyperspectral Images. IEEE Geoscience and Remote Sensing Letters, 2014, 11, 342-346.	3.1	58
183	Automatic retinal vessel extraction based on directional mathematical morphology and fuzzy classification. Pattern Recognition Letters, 2014, 47, 164-171.	4.2	97
184	Advances in Hyperspectral Image Classification: Earth Monitoring with Statistical Learning Methods. IEEE Signal Processing Magazine, 2014, 31, 45-54.	5.6	580
185	Spectral–Spatial Hyperspectral Image Classification via Multiscale Adaptive Sparse Representation. IEEE Transactions on Geoscience and Remote Sensing, 2014, 52, 7738-7749.	6.3	286
186	Multilevel Image Segmentation Based on Fractional-Order Darwinian Particle Swarm Optimization. IEEE Transactions on Geoscience and Remote Sensing, 2014, 52, 2382-2394.	6.3	212
187	Automatic Spectral–Spatial Classification Framework Based on Attribute Profiles and Supervised Feature Extraction. IEEE Transactions on Geoscience and Remote Sensing, 2014, 52, 5771-5782.	6.3	100
188	Pansharpening With Matting Model. IEEE Transactions on Geoscience and Remote Sensing, 2014, 52, 5088-5099.	6.3	94
189	Pansharpening Based on Intrinsic Image Decomposition. Sensing and Imaging, 2014, 15, 1.	1.5	5
190	Automatic Framework for Spectral–Spatial Classification Based on Supervised Feature Extraction and Morphological Attribute Profiles. IEEE Journal of Selected Topics in Applied Earth Observations and Remote Sensing, 2014, 7, 2147-2160.	4.9	101
191	Accurate point matching based on multi-objective Genetic Algorithm for multi-sensor satellite imagery. Applied Mathematics and Computation, 2014, 236, 546-564.	2.2	25
192	Feature Extraction of Hyperspectral Images With Image Fusion and Recursive Filtering. IEEE Transactions on Geoscience and Remote Sensing, 2014, 52, 3742-3752.	6.3	248
193	Remotely Sensed Image Classification Using Sparse Representations of Morphological Attribute Profiles. IEEE Transactions on Geoscience and Remote Sensing, 2014, 52, 5122-5136.	6.3	157
194	Spectral–Spatial Classification of Hyperspectral Images Based on Hidden Markov Random Fields. IEEE Transactions on Geoscience and Remote Sensing, 2014, 52, 2565-2574.	6.3	159
195	A Study on the Effectiveness of Different Independent Component Analysis Algorithms for Hyperspectral Image Classification. IEEE Journal of Selected Topics in Applied Earth Observations and Remote Sensing, 2014, 7, 2183-2199.	4.9	47
196	Hyperspectral Image Denoising Using First Order Spectral Roughness Penalty in Wavelet Domain. IEEE Journal of Selected Topics in Applied Earth Observations and Remote Sensing, 2014, 7, 2458-2467.	4.9	63
197	Feature selection of hyperspectral data by considering the integration of Genetic Algorithms and Particle Swarm Optimization. , 2014, , .		1
198	FODSPO based feature selection for hyperspectral remote sensing data. , 2014, , .		0

#	Article	IF	CITATIONS
199	Decision Fusion, Classification of Multisource Data. Encyclopedia of Earth Sciences Series, 2014, , 140-144.	0.1	3
200	A Novel Technique for Optimal Feature Selection in Attribute Profiles Based on Genetic Algorithms. IEEE Transactions on Geoscience and Remote Sensing, 2013, 51, 3514-3528.	6.3	105
201	Generalized Composite Kernel Framework for Hyperspectral Image Classification. IEEE Transactions on Geoscience and Remote Sensing, 2013, 51, 4816-4829.	6.3	439
202	Extraction of spatial features in hyperspectral images based on the analysis of differential attribute profiles. Proceedings of SPIE, 2013, , .	0.8	2
203	Hyperspectral image restoration using wavelets. Proceedings of SPIE, 2013, , .	0.8	4
204	Wavelet based hyperspectral image restoration using spatial and spectral penalties. Proceedings of SPIE, 2013, , .	0.8	7
205	Classification of hyperspectral images with binary fractional order Darwinian PSO and random forests. Proceedings of SPIE, 2013, , .	0.8	17
206	Hyperspectral Unmixing on GPUs and Multi-Core Processors: A Comparison. IEEE Journal of Selected Topics in Applied Earth Observations and Remote Sensing, 2013, 6, 1386-1398.	4.9	73
207	Sparse representation of hyperspectral data using CUR matrix decomposition. , 2013, , .		0
208	Spectral Derivative Features for Classification of Hyperspectral Remote Sensing Images: Experimental Evaluation. IEEE Journal of Selected Topics in Applied Earth Observations and Remote Sensing, 2013, 6, 594-601.	4.9	34
209	Pansharpening of remote sensing images with a matting model. , 2013, , .		2
210	Unsupervised methods for the classification of hyperspectral images with low spatial resolution. Pattern Recognition, 2013, 46, 1556-1568.	8.1	61
211	Adaptive Markov Random Fields for Joint Unmixing and Segmentation of Hyperspectral Images. IEEE Transactions on Image Processing, 2013, 22, 5-16.	9.8	51
212	Automatic Generation of Standard Deviation Attribute Profiles for Spectral–Spatial Classification of Remote Sensing Data. IEEE Geoscience and Remote Sensing Letters, 2013, 10, 293-297.	3.1	106
213	Land-Cover Mapping by Markov Modeling of Spatial–Contextual Information in Very-High-Resolution Remote Sensing Images. Proceedings of the IEEE, 2013, 101, 631-651.	21.3	200
214	Advances in Spectral-Spatial Classification of Hyperspectral Images. Proceedings of the IEEE, 2013, 101, 652-675.	21.3	1,082
215	Semisupervised Self-Learning for Hyperspectral Image Classification. IEEE Transactions on Geoscience and Remote Sensing, 2013, 51, 4032-4044.	6.3	164
216	Parsimonious Mahalanobis kernel for the classification of high dimensional data. Pattern Recognition, 2013, 46, 845-854.	8.1	27

217 Pendharpening via sparsity optimization using overcomplete transforms, 2013, 13 218 Hyperspectral image denoising using a new linear model and Sparse Regularization, 2013, 13 219 Change Detection in VHR Images Based on Morphological Attribute Profiles. IEEE Coostence and an gene transformation in the sparse Sensing Letters, 2013, 10, 656-640. 2 210 Spectral-spatial classification based on Integrated segmentation, 2013, 2 211 The spectral inguited densilication of hyperspectral images based on Hidden Mankov Rendom Field and instead and Sparse Regularization, 2013, 6 212 Smooth spectral unmixing using total variation regularization and a first order roughness penalty 6 213 Shooth spectral unmixing using total variation regularization and a first order roughness penalty 6 214 Absorces in Very-High-Resolution Remote Sensing [Scanning the Issue]. Proceedings of the IEEE, 2013, 21.3 40 215 Accomparative study of different ICA algorithms for hyperspectral image analysis, 2013, 6 216 Extending the fractional order Dorosinan particle sowarm optimization to segmentation of 0.8 11 217 Comparative study of different ICA algorithms for hyperspectral unsign initial change mask, 2012, 3 3 218 Extending the fractional order Dorosina	#	Article	IF	CITATIONS
219 Change Detection In VHR Images Based on Morphological Attribute Profiles. IEEE Geoscience and 3.1 92 220 Spectral-spatial classification based on integrated segmentation., 2013, 2 221 The spectral-spatial classification of hyperspectral images based on Hidden Markov Random Field and 10 222 Smooth spectral unmixing using total variation regularization and a first order roughness penalty., 6 223 Pate opening. IEEE Journal of Selected Topics in Applied Earth Observations and Remote Sensing. 2013, 4.9 15 224 Advances in Very-High-Resolution Remote Sensing [Scanning the Issue]. Proceedings of the IEEE, 2013, 21.3 40 225 Extending the fractional order Darwinian particle swarm optimization to segmentation of Myperspectral Images. Proceedings of the IEEE, 2013, 21.3 40 226 Extending the fractional order Darwinian particle swarm optimization to segmentation of Myperspectral Images. Proceedings of SPIE, 2012, 4 227 Comparison of HIPCA and IRMAD for automatic change detection using Initial change mask, 2012, 3 228 Anew pansharpening method using an explicit Image formation model regularized via Total Variation., 5 229 Classification of hyperspectral Images based on weighted DMPS., 2012, 3 230 Hyperspectral Image	217	Pansharpening via sparsity optimization using overcomplete transforms. , 2013, , .		2
219 Remote Sensing Letters, 2013, 10, 636-640. 51 92 220 Spectral-spatial classification based on integrated segmentation., 2013, , . 2 221 The spectral-spatial classification of hyperspectral images based on Hidden Markov Random Field and the Expectation-Maximization., 2013, 10 222 Smooth spectral unmixing using total variation regularization and a first order roughness penalty., 2013,	218	Hyperspectral image denoising using a new linear model and Sparse Regularization. , 2013, , .		13
221 The spectral-spectial classification of hyperspectral images based on Hidden Markov Random Field and 10 222 Smooth spectral unmixing using total variation regularization and a first order roughness penalty., 6 223 Path Opening, IEE Journal of Selected Topics in Applied Earth Observations and Remote Sensing, 2013, 4.9 15 224 Advances in Very-High-Resolution Remote Sensing [Scanning the Issue]. Proceedings of the IEEE, 2013, 21.3 40 225 A comparative study of different ICA algorithms for hyperspectral image analysis., 2013, 4 1 226 Extending the fractional order Darwinian particle swarm optimization to segmentation of hyperspectral images. Proceedings of SPIE, 2012, 0.8 11 227 Comparison of ITPCA and IRMAD for automatic change detection using Initial change mask., 2012, 3 3 228 Anew pansharpening method using an explicit image formation model regularized via Total Variation., 2012, 3 230 Hyperspectral images denoising using 3D wavelets., 2012, 49 231 Input-output-consistent domain adaptation algorithm for remote sensing data classification., 2012, 1 231 Input-output-consistent domain adaptation algorithm for remote sensing data classification., 2012, 1 232 Lease detection using l	219		3.1	92
211 Its Expectation-Maximization , 2013, 10 222 Smooth spectral unnixing using total variation regularization and a first order roughness penalty., 6 223 Detection of Hedges in a Rural Landscape Using a Local Orientation Feature: From Linear Opening to 4.9 15 224 Advances in Very-High-Resolution Remote Sensing [Scanning the Issue]. Proceedings of the IEEE, 2013, 21.3 40 225 A comparative study of different ICA algorithms for hyperspectral image analysis., 2013, 4 226 Extending the fractional order Darwinian particle swarm optimization to segmentation of hyperspectral images. Proceedings of SPIE, 2012, 3 227 Comparison of ITPCA and IRMAD for automatic change detection using initial change mask., 2012, 3 228 Anew pansharpening method using an explicit image formation model regularized via Total Variation., 2012, 5 229 Classification of hyperspectral images based on weighted DMPS., 2012, 3 230 Hyperspectral image denoising using 3D wavelets., 2012, 4 231 Input-output-consistent domain adaptation algorithm for remote sensing data classification., 2012, 1 231 Hyperspectral image detection algorithm for remote sensing data classification., 2012, 1 232 Hedges detection using local	220	Spectral-spatial classification based on integrated segmentation. , 2013, , .		2
222 2013,	221			10
223 Path Opening, IEEE Journal of Selected Topics in Applied Earth Observations and Remote Sensing, 2013, 4.9 15 224 Advances in Very-High-Resolution Remote Sensing [Scanning the Issue]. Proceedings of the IEEE, 2013, 21.3 40 225 A comparative study of different ICA algorithms for hyperspectral image analysis., 2013, 4 226 Extending the fractional order Darwinian particle swarm optimization to segmentation of hyperspectral images. Proceedings of SPIE, 2012, , 0.8 11 227 Comparison of ITPCA and IRMAD for automatic change detection using initial change mask., 2012, , 3 228 Anew pansharpening method using an explicit image formation model regularized via Total Variation., 2012, , 5 229 Classification of hyperspectral images based on weighted DMPS., 2012, , 3 230 Hyperspectral image denoising using 3D wavelets., 2012, , 4 231 Input-output-consistent domain adaptation algorithm for remote sensing data classification., 2012, , 1 232 Hedges detection using local directional features and support vector data description., 2012, , 2	222			6
224 101, 566-569. 21.3 40 225 A comparative study of different ICA algorithms for hyperspectral image analysis. , 2013, , . 4 226 Extending the fractional order Darwinian particle swarm optimization to segmentation of hyperspectral images. Proceedings of SPIE, 2012, , . 0.8 11 227 Comparison of ITPCA and IRMAD for automatic change detection using initial change mask. , 2012, , . 3 228 A new pansharpening method using an explicit image formation model regularized via Total Variation. , 2012, , . 5 229 Classification of hyperspectral images based on weighted DMPS. , 2012, , . 3 230 Hyperspectral image denoising using 3D wavelets. , 2012, , . 49 231 Input-output-consistent domain adaptation algorithm for remote sensing data classification. , 2012, , . 1 232 Hedges detection using local directional features and support vector data description. , 2012, , . 2	223	Path Opening. IEEE Journal of Selected Topics in Applied Earth Observations and Remote Sensing, 2013,	4.9	15
226Extending the fractional order Darwinian particle swarm optimization to segmentation of hyperspectral images. Proceedings of SPIE, 2012, ,.0.811227Comparison of ITPCA and IRMAD for automatic change detection using initial change mask. , 2012, ,.3228A new pansharpening method using an explicit image formation model regularized via Total Variation. , 2012, ,.5229Classification of hyperspectral images based on weighted DMPS. , 2012, ,.3230Hyperspectral image denoising using 3D wavelets. , 2012, ,.49231Input-output-consistent domain adaptation algorithm for remote sensing data classification. , 2012, ,.1232Hedges detection using local directional features and support vector data description. , 2012, ,.2	224		21.3	40
226 hyperspectral images. Proceedings of SPIE, 2012, ,	225	A comparative study of different ICA algorithms for hyperspectral image analysis. , 2013, , .		4
228A new pansharpening method using an explicit image formation model regularized via Total Variation., 2012,,.5229Classification of hyperspectral images based on weighted DMPS., 2012,,.3230Hyperspectral image denoising using 3D wavelets., 2012,,.49231Input-output-consistent domain adaptation algorithm for remote sensing data classification., 2012,,.1232Hedges detection using local directional features and support vector data description., 2012,,.2	226		0.8	11
228 2012, , . 1 229 Classification of hyperspectral images based on weighted DMPS., 2012, , . 3 230 Hyperspectral image denoising using 3D wavelets., 2012, , . 49 231 Input-output-consistent domain adaptation algorithm for remote sensing data classification., 2012, , . 1 232 Hedges detection using local directional features and support vector data description., 2012, , . 2	227	Comparison of ITPCA and IRMAD for automatic change detection using initial change mask. , 2012, , .		3
230Hyperspectral image denoising using 3D wavelets., 2012,,.49231Input-output-consistent domain adaptation algorithm for remote sensing data classification., 2012,,.1232Hedges detection using local directional features and support vector data description., 2012,,.2	228			5
231 Input-output-consistent domain adaptation algorithm for remote sensing data classification., 2012, , . 1 232 Hedges detection using local directional features and support vector data description., 2012, , . 2	229	Classification of hyperspectral images based on weighted DMPS. , 2012, , .		3
Hedges detection using local directional features and support vector data description., 2012, , . 2	230	Hyperspectral image denoising using 3D wavelets. , 2012, , .		49
	231	Input-output-consistent domain adaptation algorithm for remote sensing data classification. , 2012, , .		1
A smooth hyperspectral unmixing method using cyclic descent. , 2012, , . 4	232	Hedges detection using local directional features and support vector data description. , 2012, , .		2
	233	A smooth hyperspectral unmixing method using cyclic descent. , 2012, , .		4

234 Detection of hedges based on attribute filters. , 2012, , .

#	Article	IF	CITATIONS
235	Spectral unmixing of multispectral satellite images with dimensionality expansion using morphological profiles. , 2012, , .		6
236	Very High-Resolution Remote Sensing: Challenges and Opportunities [Point of View]. Proceedings of the IEEE, 2012, 100, 1907-1910.	21.3	84
237	SAR image denoising using total variation based regularization with sure-based optimization of the regularization parameter. , 2012, , .		11
238	Spectral derivative features for supervised classification of remote sensing data: An experimental evaluation. , 2012, , .		0
239	Markov random field models for supervised land cover classification from very high resolution multispectral remote sensing images. , 2012, , .		4
240	An efficient method for segmentation of images based on fractional calculus and natural selection. Expert Systems With Applications, 2012, 39, 12407-12417.	7.6	251
241	A new parallel tool for classification of remotely sensed imagery. Computers and Geosciences, 2012, 46, 208-218.	4.2	26
242	Classification of Remote Sensing Optical and LiDAR Data Using Extended Attribute Profiles. IEEE Journal on Selected Topics in Signal Processing, 2012, 6, 856-865.	10.8	139
243	A novel supervised feature selection technique based on genetic algorithms. , 2012, , .		6
244	Classification of hyperspectral data using extended attribute profiles based on supervised and unsupervised feature extraction techniques. International Journal of Image and Data Fusion, 2012, 3, 269-298.	1.7	54
245	A spatial–spectral kernel-based approach for the classification of remote-sensing images. Pattern Recognition, 2012, 45, 381-392.	8.1	245
246	A Marker-Based Approach for the Automated Selection of a Single Segmentation From a Hierarchical Set of Image Segmentations. IEEE Journal of Selected Topics in Applied Earth Observations and Remote Sensing, 2012, 5, 262-272.	4.9	70
247	Classification of Pansharpened Urban Satellite Images. IEEE Journal of Selected Topics in Applied Earth Observations and Remote Sensing, 2012, 5, 281-297.	4.9	69
248	Retrieval of the Height of Buildings From WorldView-2 Multi-Angular Imagery Using Attribute Filters and Geometric Invariant Moments. IEEE Journal of Selected Topics in Applied Earth Observations and Remote Sensing, 2012, 5, 71-79.	4.9	37
249	Automatic Extraction of Ellipsoidal Features for Planetary Image Registration. IEEE Geoscience and Remote Sensing Letters, 2012, 9, 95-99.	3.1	39
250	Linear Versus Nonlinear PCA for the Classification of Hyperspectral Data Based on the Extended Morphological Profiles. IEEE Geoscience and Remote Sensing Letters, 2012, 9, 447-451.	3.1	273
251	Spectral–Spatial Classification of Hyperspectral Data Based on a Stochastic Minimum Spanning Forest Approach. IEEE Transactions on Image Processing, 2012, 21, 2008-2021.	9.8	107
252	Extended morphological profiles using auto-associative neural networks for hyperspectral data classification. , 2011, , .		4

#	Article	IF	CITATIONS
253	A Stochastic Minimum Spanning Forest approach for spectral-spatial classification of hyperspectral images. , 2011, , .		4
254	Hyperspectral Image Classification With Independent Component Discriminant Analysis. IEEE Transactions on Geoscience and Remote Sensing, 2011, 49, 4865-4876.	6.3	325
255	Hyperspectral change detection using IR-MAD and feature reduction. , 2011, , .		10
256	The Evolution of the Morphological Profile: from Panchromatic to Hyperspectral Images. , 2011, , 123-146.		16
257	Classification using Extended Morphological Attribute Profiles based on different feature extraction techniques. , 2011, , .		8
258	Greetings from GRSS president. , 2011, , .		0
259	Spectral-spatial classification of polarimetric SAR data using morphological attribute profiles. Proceedings of SPIE, 2011, , .	0.8	11
260	A Parallel Simulated Annealing Approach to Band Selection for High-Dimensional Remote Sensing Images. IEEE Journal of Selected Topics in Applied Earth Observations and Remote Sensing, 2011, 4, 579-590.	4.9	26
261	Spectral Unmixing for the Classification of Hyperspectral Images at a Finer Spatial Resolution. IEEE Journal on Selected Topics in Signal Processing, 2011, 5, 521-533.	10.8	139
262	Introduction to the Issue on Advances in Remote Sensing Image Processing. IEEE Journal on Selected Topics in Signal Processing, 2011, 5, 365-369.	10.8	22
263	Classification of Hyperspectral Images by Using Extended Morphological Attribute Profiles and Independent Component Analysis. IEEE Geoscience and Remote Sensing Letters, 2011, 8, 542-546.	3.1	340
264	Unsupervised classification and spectral unmixing for sub-pixel labelling. , 2011, , .		3
265	Marker-based Hierarchical Segmentation and classification approach for hyperspectral imagery. , 2011,		6
266	Joint spectral classification and unmixing using adaptative pixel neighborhoods. , 2011, , .		0
267	Scalable semi-supervised classification of hyperspectral remote sensing data with spectral and spatial information. , 2011, , .		3
268	A general approach to the spatial simplification of remote sensing images based on morphological connected filters. , 2011, , .		1
269	Fusion of hyperspectral and lidar data using morphological attribute profiles. , 2011, , .		3
270	Urban area product simulation for the EnMap hyperspectral sensor. , 2011, , .		0

#	Article	IF	CITATIONS
271	Mahalanobis kernel based on probabilistic principal component. , 2011, , .		0
272	Unsupervised Change Detection in Multitemporal Images of the Human Retina. , 2011, , 309-337.		1
273	Hierarchical Analysis of Remote Sensing Data: Morphological Attribute Profiles and Binary Partition Trees. Lecture Notes in Computer Science, 2011, , 306-319.	1.3	11
274	Self-dual Attribute Profiles for the Analysis of Remote Sensing Images. Lecture Notes in Computer Science, 2011, , 320-330.	1.3	27
275	Supervised super-resolution to improve the resolution of hyperspectral images classification maps. Proceedings of SPIE, 2010, , .	0.8	3
276	Sensitivity of Support Vector Machines to Random Feature Selection in Classification of Hyperspectral Data. IEEE Transactions on Geoscience and Remote Sensing, 2010, 48, 2880-2889.	6.3	263
277	Morphological Attribute Profiles for the Analysis of Very High Resolution Images. IEEE Transactions on Geoscience and Remote Sensing, 2010, 48, 3747-3762.	6.3	626
278	Multiple Spectral–Spatial Classification Approach for Hyperspectral Data. IEEE Transactions on Geoscience and Remote Sensing, 2010, , .	6.3	150
279	SVM- and MRF-Based Method for Accurate Classification of Hyperspectral Images. IEEE Geoscience and Remote Sensing Letters, 2010, 7, 736-740.	3.1	651
280	Segmentation and classification of hyperspectral images using watershed transformation. Pattern Recognition, 2010, 43, 2367-2379.	8.1	506
281	Advanced directional mathematical morphology for the detection of the road network in very high resolution remote sensing images. Pattern Recognition Letters, 2010, 31, 1120-1127.	4.2	210
282	Mahalanobis kernel for the classification of hyperspectral images. , 2010, , .		7
283	Extended profiles with morphological attribute filters for the analysis of hyperspectral data. International Journal of Remote Sensing, 2010, 31, 5975-5991.	2.9	339
284	Super-resolution: an efficient method to improve spatial resolution of hyperspectral images. , 2010, , .		13
285	A classifier ensemble based on fusion of support vector machines for classifying hyperspectral data. International Journal of Image and Data Fusion, 2010, 1, 293-307.	1.7	89
286	Crater detection based on marked point processes. , 2010, , .		6
287	On the influence of feature reduction for the classification of hyperspectral images based on the extended morphological profile. International Journal of Remote Sensing, 2010, 31, 5921-5939.	2.9	36
288	Study on the capabilities of morphological attribute profiles in change detection on VHR images. ,		4

Study on 2010, , . 288

#	Article	IF	CITATIONS
289	Alternating sequential filters with morphological attribute operators for the analysis of remote sensing images. , 2010, , .		3
290	Segmentation and Classification of Hyperspectral Images Using Minimum Spanning Forest Grown From Automatically Selected Markers. IEEE Transactions on Systems, Man, and Cybernetics, 2010, 40, 1267-1279.	5.0	250
291	Classification of hyperspectral images with Extended Attribute Profiles and feature extraction techniques. , 2010, , .		20
292	A multiple classifier approach for spectral-spatial classification of hyperspectral data. , 2010, , .		20
293	Independent Component Discriminant Analysis for hyperspectral image classification. , 2010, , .		8
294	Image fusion for classification of high resolution images based on mathematical morphology. , 2010, , .		1
295	Classification of hyperspectral images by using morphological attribute filters and Independent Component Analysis. , 2010, , .		1
296	Algorithms and Applications for Land Cover Classification $\hat{a} \in \hat{A}$ Review. , 2010, , 203-233.		2
297	Band selection for hyperspectral images based on parallel particle swarm optimization schemes. , 2009, , .		15
298	Automatic Extraction of Planetary Image Features. , 2009, , .		2
299	Glaucoma Filtration Surgery and Retinal Oxygen Saturation. , 2009, 50, 5247.		45
300	Kernel principal component analysis for the construction of the extended morphological profile. , 2009, , .		1
301	Ensemble Strategies for Classifying Hyperspectral Remote Sensing Data. Lecture Notes in Computer Science, 2009, , 62-71.	1.3	7
302	On the use of ICA for hyperspectral image analysis. , 2009, , .		26
303	Oxygen Saturation in Human Retinal Vessels Is Higher in Dark Than in Light. , 2009, 50, 2308.		82
304	Ensemble Classification Algorithm for Hyperspectral Remote Sensing Data. IEEE Geoscience and Remote Sensing Letters, 2009, 6, 762-766.	3.1	46
305	Recent advances in techniques for hyperspectral image processing. Remote Sensing of Environment, 2009, 113, S110-S122.	11.0	1,452
306	Impact of different morphological profiles on the classification accuracy of urban hyperspectral		3

data. , 2009, , .

#	Article	IF	CITATIONS
307	Classification based marker selection for watershed transform of hyperspectral images. , 2009, , .		13
308	Morphological attribute filters for the analysis of very high resolution remote sensing images. , 2009, , .		11
309	Directional mathematical morphology for the detection of the road network in Very High Resolution remote sensing images. , 2009, , .		3
310	Spectral–Spatial Classification of Hyperspectral Imagery Based on Partitional Clustering Techniques. IEEE Transactions on Geoscience and Remote Sensing, 2009, 47, 2973-2987.	6.3	590
311	Classification of hyperspectral images using automatic marker selection and Minimum Spanning Forest. , 2009, , .		4
312	Ensemble methods for spectral-spatial classification of urban hyperspectral data. , 2009, , .		7
313	Mapping of hyperspectral AVIRIS data using machine-learning algorithms. Canadian Journal of Remote Sensing, 2009, 35, S106-S116.	2.4	120
314	Modeling structural information for building extraction with morphological attribute filters. Proceedings of SPIE, 2009, , .	0.8	13
315	Speckle reduction of TerraSAR-X imagery using TV segmentation. , 2009, , .		Ο
316	Speckle reduction of SAR images using sure-based adaptive Sigmoid thresholding in the wavelet domain. , 2009, , .		6
317	Fusion of multisource data sets from agricultural areas for improved land cover classification. , 2009, , .		2
318	Kernel Principal Component Analysis for the Classification of Hyperspectral Remote Sensing Data over Urban Areas. Eurasip Journal on Advances in Signal Processing, 2009, 2009, .	1.7	207
319	Classifying Remote Sensing Data with Support Vector Machines and Imbalanced Training Data. Lecture Notes in Computer Science, 2009, , 375-384.	1.3	21
320	Hierarchical Ensemble Support Cluster Machine. Lecture Notes in Computer Science, 2009, , 252-261.	1.3	0
321	Retinal oxygenation in diabetic retinopathy. Acta Ophthalmologica, 2009, 87, 0-0.	1.1	0
322	Michael J. Barnsley. IEEE Transactions on Geoscience and Remote Sensing, 2008, 46, 303-303.	6.3	0
323	Model-Based Satellite Image Fusion. IEEE Transactions on Geoscience and Remote Sensing, 2008, 46, 1336-1346.	6.3	58
324	On the decomposition of Mars hyperspectral data by ICA and Bayesian positive source separation. Neurocomputing, 2008, 71, 2194-2208.	5.9	121

#	ARTICLE	IF	CITATIONS
325	Spectral and Spatial Classification of Hyperspectral Data Using SVMs and Morphological Profiles. IEEE Transactions on Geoscience and Remote Sensing, 2008, 46, 3804-3814.	6.3	930
326	An Unsupervised Technique Based on Morphological Filters for Change Detection in Very High Resolution Images. IEEE Geoscience and Remote Sensing Letters, 2008, 5, 433-437.	3.1	106
327	Automatic registration of retina images based on genetic techniques. , 2008, 2008, 5419-24.		10
328	Adaptive pixel neighborhood definition for the classification of hyperspectral images with support vector machines and composite kernel. , 2008, , .		19
329	Combined Wavelet and Contourlet Denoising of SAR Images. , 2008, , .		12
330	Spectrally Consistent Pansharpening. , 2008, , 293-311.		1
331	Ensemble Methods for Classification of Hyperspectral Data. , 2008, , .		11
332	Gradient Optimization for multiple kernel's parameters in support vector machines classification. , 2008, , .		23
333	Speckle Reduction of SAR Images in the Bandlet Domain. , 2008, , .		3
334	Segmentation and Classification of Hyperspectral Data using Watershed. , 2008, , .		41
335	Cluster-Based Ensemble Classification for Hyperspectral Remote Sensing Images. , 2008, , .		13
336	Semi-Supervised Classifier Ensembles for Classifying Remote Sensing Data. , 2008, , .		2
337	Shadow extraction. Journal of Physics: Conference Series, 2008, 139, 012032.	0.4	1
338	Spectral and spatial classification of hyperspectral data using SVMs and morphological profiles. , 2007, , .		64
339	European perspectives in hyperspectral data analysis. , 2007, , .		9
340	A joint spatial and spectral SVM's classification of panchromatic images. , 2007, , .		6
341	A Novel Technique Based on Morphological Filters for Change Detection in Optical Remote Sensing Images. AIP Conference Proceedings, 2007, , .	0.4	2
342	HYPER-I-NET: European research network on hyperspectral imaging. , 2007, , .		4

#	Article	IF	CITATIONS
343	Fusion of support vector machines for classifying SAR and multispectral imagery from agricultural areas. , 2007, , .		6
344	How Transferable Are Spatial Features for the Classification of Very High Resolution Remote Sensing Data?. , 2007, , .		0
345	On spatial priors for satellite image fusio. , 2007, , .		0
346	Random Forest Classification of Remote Sensing Data. , 2007, , 61-78.		2
347	Multiple Classifier Systems in Remote Sensing: From Basics to Recent Developments. , 2007, , 501-512.		91
348	Smoothing of fused spectral consistent satellite images with TV-based edge detection. , 2007, , .		1
349	Combined wavelet and curvelet denoising of SAR images using TV segmentation. , 2007, , .		17
350	Fusion of Support Vector Machines for Classification of Multisensor Data. IEEE Transactions on Geoscience and Remote Sensing, 2007, 45, 3858-3866.	6.3	329
351	Classification of Remote Sensing Images From Urban Areas Using a Fuzzy Possibilistic Model. IEEE Geoscience and Remote Sensing Letters, 2006, 3, 40-44.	3.1	106
352	Spectrally Consistent Satellite Image Fusion with Improved Image Priors. , 2006, , .		3
353	Feature Selection for Morphological Feature Extraction using Randomforests. , 2006, , .		5
354	Unsupervised Change-Detection in Color Fundus Images of the Human Retina. , 2006, , .		2
355	Decision Fusion for the Classification of Urban Remote Sensing Images. IEEE Transactions on Geoscience and Remote Sensing, 2006, 44, 2828-2838.	6.3	205
356	Automatic Retinal Oximetry. , 2006, 47, 5011.		241
357	Random Forests for land cover classification. Pattern Recognition Letters, 2006, 27, 294-300.	4.2	1,610
358	The Physical Meaning of Independent Components and Artifact Removal of Hyperspectral Data from Mars using ICA. , 2006, , .		1
359	Combined Curvelet and Wavelet Denoising. , 2006, , .		3

360 Smoothing of Fused Spectral Consistent Satellite Images. , 2006, , .

1

#	Article	IF	CITATIONS
361	Feature Selection for Morphological Feature Extraction using Random Forests. , 2006, , .		3
362	A Combined Support Vector Machines Classification Based on Decision Fusion. , 2006, , .		18
363	Kernel Principal Component Analysis for Feature Reduction in Hyperspectrale Images Analysis. , 2006, , .		39
364	Advanced processing of hyperspectral images. , 2006, , .		20
365	Fusion of Morphological and Spectral Information for Classification of Hyperspectal Urban Remote Sensing Data. , 2006, , .		12
366	Classification of hyperspectral data from urban areas based on extended morphological profiles. IEEE Transactions on Geoscience and Remote Sensing, 2005, 43, 480-491.	6.3	1,189
367	Exploiting Spectral and Spatial Information in Hyperspectral Urban Data With High Resolution. IEEE Geoscience and Remote Sensing Letters, 2004, 1, 322-326.	3.1	196
368	Foreword to the special issue on urban remote sensing by satellite. IEEE Transactions on Geoscience and Remote Sensing, 2003, 41, 1903-1906.	6.3	11
369	Multisource remote sensing data classification based on consensus and pruning. IEEE Transactions on Geoscience and Remote Sensing, 2003, 41, 932-936.	6.3	49
370	Classification and feature extraction for remote sensing images from urban areas based on morphological transformations. IEEE Transactions on Geoscience and Remote Sensing, 2003, 41, 1940-1949.	6.3	642
371	Almost translation invariant wavelet transformations for speckle reduction of sar images. IEEE Transactions on Geoscience and Remote Sensing, 2003, 41, 2404-2408.	6.3	42
372	Data fusion and feature extraction in the wavelet domain. International Journal of Remote Sensing, 2003, 24, 3933-3945.	2.9	22
373	Image Segmentation Based on the Derivative of the Morphological Profile. , 2002, , 179-188.		7
374	<title>Review of applications of wavelets in speckle reduction and enhancement of SAR images</title> . , 2002, 4541, 47.		2
375	Multiple classifiers applied to multisource remote sensing data. IEEE Transactions on Geoscience and Remote Sensing, 2002, 40, 2291-2299.	6.3	244
376	Correction to "The effect of classifier agreement on the accuracy of the combined classifier in decision level fusion". IEEE Transactions on Geoscience and Remote Sensing, 2002, 40, 228-228.	6.3	1
377	A new approach for the morphological segmentation of high-resolution satellite imagery. IEEE Transactions on Geoscience and Remote Sensing, 2001, 39, 309-320.	6.3	715
378	The effect of classifier agreement on the accuracy of the combined classifier in decision level fusion. IEEE Transactions on Geoscience and Remote Sensing, 2001, 39, 2539-2546.	6.3	64

#	Article	IF	CITATIONS
379	Consensus Based Classification of Multisource Remote Sensing Data. Lecture Notes in Computer Science, 2000, , 280-289.	1.3	7
380	Classification of multisource and hyperspectral data based on decision fusion. IEEE Transactions on Geoscience and Remote Sensing, 1999, 37, 1367-1377.	6.3	223
381	<title>Neuro-fuzzy and soft computing in classification of remote sensing data</title> . , 1999, , .		1
382	<title>Speckle reduction and enhancement of SAR images using multiwavelets and adaptive thresholding</title> . , 1999, , .		11
383	STATISTICAL AND NEURAL NETWORK PATTERN RECOGNITION METHODS FOR REMOTE SENSING APPLICATIONS. , 1999, , 507-534.		2
384	An extension of parametric decision boundary feature extraction (DBFE) for classification of hyperdimensional data. , 1998, , .		0
385	Classification and integration of multitype data. , 1998, , .		1
386	<title>Optimized combination, regularization, and pruning in parallel consensual neural networks</title> . , 1998, , .		1
387	Translation invariant wavelets for speckle reduction of SAR images. , 1998, , .		1
388	Feature extraction based on LOOC estimation. , 1998, , .		0
389	Feature extraction for multisource data classification with artificial neural networks. International Journal of Remote Sensing, 1997, 18, 727-740.	2.9	96
390	Parallel consensual neural networks. IEEE Transactions on Neural Networks, 1997, 8, 54-64.	4.2	151
391	Hybrid consensus theoretic classification. IEEE Transactions on Geoscience and Remote Sensing, 1997, 35, 833-843.	6.3	95
392	Parallel principal component neural networks for classification of event-related potential waveforms. Medical Engineering and Physics, 1997, 19, 15-20.	1.7	20
393	Multistage classifiers optimized by neural networks and genetic algorithms. Nonlinear Analysis: Theory, Methods & Applications, 1997, 30, 1323-1334.	1.1	12
394	Classification and feature extraction of AVIRIS data. IEEE Transactions on Geoscience and Remote Sensing, 1995, 33, 1194-1205.	6.3	79
395	Conjugate-gradient neural networks in classification of multisource and very-high-dimensional remote sensing data. International Journal of Remote Sensing, 1993, 14, 2883-2903.	2.9	99
396	Consensus theoretic classification methods. IEEE Transactions on Systems, Man, and Cybernetics, 1992, 22, 688-704.	0.9	298

#	Article	IF	CITATIONS
397	Neural Network Approaches Versus Statistical Methods In Classification Of Multisource Remote Sensing Data. IEEE Transactions on Geoscience and Remote Sensing, 1990, 28, 540-552.	6.3	757
398	Decision level fusion of multitype data. , 0, , .		3
399	An investigation of multiple self-organizing feature maps for classification of multisource data. , 0, , .		0
400	Neural Network Approaches Versus Statistical Methods in Classification of Multisource Remote Sensing Data. , 0, , .		20
401	a Method of Statistical Multisource Classification with a Mechanism to WeIght the Influence of the Data Sources. , 0, , .		12
402	Classification Of Very High Dimensional Data Using Neural Networks. , 0, , .		11
403	A Consensual Neural Network. , 0, , .		3
404	Feature Selection For Neural Networks Using Parzen Density Estimator. , 0, , .		0
405	Parallel consensual neural networks. , 0, , .		6
406	Classification of event-related potential waveforms with parallel principal component neural networks. , 0, , .		0
407	Speckle reduction and enhancement of SAR images in the wavelet domain. , 0, , .		33
408	Optimized consensus theory. , 0, , .		0
409	Optimized combination of neural networks. , 0, , .		2
410	Hybrid consensus theoretic classification. , 0, , .		4
411	Classification and feature extraction with enhanced statistics. , 0, , .		3
412	Wavelet-package transformation as a preprocessor of EEG waveforms for classification. , 0, , .		6
413	Classification of hyperdimensional data using data fusion approaches. , 0, , .		3

#	Article	IF	CITATIONS
415	Feature extraction for neural network classifiers using wavelets and tree structured filter banks. , 0, , .		1
416	Classification and feature extraction of hyperdimensional data using LOOC covariance estimation. , 0, , .		1
417	Cancellation of nonlinear intersymbol interference in voiceband communication channels. , 0, , .		1
418	Hybrid consensus theoretic classification with pruning and regularization. , 0, , .		2
419	Multiple wavelet transforms for speckle reduction of SAR images. , 0, , .		1
420	The effect of correlation on the accuracy of the combined classifier in decision level fusion. , 0, , .		14
421	Speckle reduction of SAR images using wavelet-domain hidden Markov models. , 0, , .		4
422	Data fusion and feature extraction using tree structured filter banks. , 0, , .		3
423	Absolute neuro-fuzzy classification of remote sensing data. , 0, , .		1
424	The use of morphological profiles in classification of data from urban areas. , 0, , .		12
425	Speckle reduction of SAR images in the complex wavelet domain. , 0, , .		2
426	Feature extraction and classification of urban high-resolution satellite imagery based on morphological preprocessing. , 0, , .		0
427	Cluster-based feature extraction and data fusion in the wavelet domain. , 0, , .		5
428	Use of multiple classifiers in classification of data from multiple data sources. , 0, , .		9
429	Speckle reduction of SAR images in the curvelet domain. , 0, , .		29
430	Morphological profiles used for classification of data from urban areas. , 0, , .		4
431	Double density wavelet transformation for speckle reduction of SAR images. , 0, , .		2

#	Article	IF	CITATIONS
433	Speckle reduction of SAR images using adaptive curvelet domain. , 0, , .		23
434	Morphological pre-processing for classification of hyperspectral data from urban areas. , 0, , .		3
435	Morphological transformations and feature extraction of urban data with high spectral and spatial resolution. , 0, , .		13
436	Wavelet footprints for speckle reduction of SAR images. , 0, , .		0
437	Support vector machines in multisource classification. , 0, , .		13
438	On the use of morphological alternated sequential filters for the classification of remote sensing images from urban areas. , 0, , .		8
439	Classification of remote sensing images from urban areas using a fuzzy model. , 0, , .		6
440	Decision level fusion in classification of hyperspectral data from urban areas. , 0, , .		2
441	Source based feature extraction for support vector machines in hyperspectral classification. , 0, , .		6
442	Combined wavelet and curvelet denoising of SAR images. , 0, , .		33
443	Random forest classification of multisource remote sensing and geographic data. , 0, , .		52
444	Fusion of methods for the classification of remote sensing images from urban areas. , 0, , .		10
445	Random forest classifiers for hyperspectral data. , 0, , .		23
446	Translation Invariant Combined Denoising Algorithm. , 0, , .		5
447	Street tracking based on SAR data from urban areas. , 0, , .		2
448	Spectral consistent satellite image fusion: using a high resolution panchromatic and low resolution multi-spectral images. , 0, , .		11
449	Classification of hyperspectral data from urban areas using morpholgical preprocessing and independent component analysis. , 0, , .		45
450	Classification of hyperspectral rosis data from urban areas. , 0, , .		5

Classification of hyperspectral rosis data from urban areas. , 0, , . 450

#	Article	IF	CITATIONS
451	Evaluation of Kernels for Multiclass Classification of Hyperspectral Remote Sensing Data. , 0, , .		65
452	Decision Fusion for Hyperspectral Classification. , 0, , 313-351.		2
453	Retinal oxygen saturation in humans in light and dark. Acta Ophthalmologica, 0, 85, 0-0.	0.3	0